Hindawi
Advances in Multimedia
Volume 2022, Article ID 7511630, 13 pages
https://doi.org/10.1155/2022/7511630

Research Article

The Promotion Effect of Computer-Aided Technology Combined with RBF Neural Network Algorithm on Art Design

Chunliang Pan[1] and Yuning Pan[2]

[1]*Weifang Engineering Vocational College, Qingzhou, Shandong 262500, China*
[2]*Shanghai University, Shanghai 20044, China*

Correspondence should be addressed to Yuning Pan; paccpyn@shu.edu.cn

Received 23 June 2022; Revised 6 July 2022; Accepted 11 July 2022; Published 6 September 2022

Academic Editor: Qiangyi Li

In order to improve the effect of fractal art pattern design, this study combines RBF neural network algorithm to design and evaluate CAD fractal art pattern to improve the effect of fractal art pattern design. Moreover, this study proposes a dynamic weight-based NSC method. Because noise is ubiquitous in reality, the evolution of system dynamics often cannot be carried out strictly according to the iterative rules. In addition, this study shows the changing rules of the competition relationship and the distribution of competitors under the interference of noise. Finally, this study controls the style of the art pattern design in the spatial domain and uses the mask image pattern to disguise the art style. The experimental study shows that the CAD fractal art pattern design system based on the RBF neural network algorithm proposed in this study has a good effect on fractal art pattern design.

1. Introduction

Digital art graphics can be created by continuous iteration of numbers and computer programs. This iteration is not only a nonlinear transformation, but can also be expressed as a process in a broad sense. The theory of fractals and their meanings have extensive and far-reaching influence, and it can be said that the idea of fractals is a worldview. It is one of the basic theories that constitute nonlinear science, and its appearance also clarifies digital art completely. For example, the famous Mandelbrot set and Julia set can generate breathtaking fine structures with the aid of computers, which have infinite possible shapes. If the geometric method of perspective projection is the first encounter between science and art, then fractal geometry can be said to be the second combination of science and art. Fractal graphics can be generated by recursive algorithm, grammar composition algorithm, iterative function system algorithm, escape time algorithm, and cell evolution algorithm [1]. These computer-generated graphics are designed in a virtual electronic space, using some abstract digital rules or databases, and are immaterial in nature. Since the appearance of this graphic generation method, it has been widely used by designers in the creation of two-dimensional and three-dimensional images and finally formed the concept of "digital art." Digital art is not only used to generate fantasy-like effects but also needs to study the characteristics of changes in the design process. This interactivity is the main difference between digital art and traditional art, and it changes the way people perceive art [2]. Moreover, digital art graphics generation technology can be used in textile printing and dyeing, industrial design or clothing design, and computer art teaching, and its economic and social benefits are obvious, and it has a very broad application prospect [3].

The computer can generate infinitely varied, mysterious, and beautiful digital art graphics through certain numerical calculation methods. These graphics have partial or overall self-similarity, dynamic balance, symmetry, and fine structure, with harmonious rhythm and unique rhythm, reflecting artistic and artistic harmony. The perfect combination of science: graphics in general concept refer to a specific type of image, its main visual feature is shape, the

outer contour lines that constitute the main body are obvious, there is no complex texture inside, and the color is simple, so general graphics can be classified or retrieved by shape features [4]. Digital art graphics [5] are generated by the computer's continuous iteration of digital rules, so it also has a certain degree of mechanical and randomness. Digital art graphics naturally have complex characteristics such as color, shape, and texture. When artists are looking for materials, they hope to find graphics in the graphics database that match their ideas and creative inspiration, but most graphics cannot automatically conform to the user's subjective thoughts and feelings [6]. Using digital image processing technology to carry out objective aesthetic evaluation and emotional retrieval of digital art graphics by computer can not only facilitate designers to select suitable graphics but also play a guiding role in graphics design and stimulate creative inspiration [7].

Fractal geometry can provide realistic descriptions for various scenes that exist in nature. The shapes of these scenes are complex and irregular. It is very rough, which makes it extremely difficult to describe with traditional geometric tools, while fractal models can describe natural scenes very well; because many actual scenes in nature are generally fractal, or vice versa, the shape constructed according to the fractal geometry method is very similar to many natural scenes [8]. Several experiments on a computer to draw self-similar sets have been able to produce surprisingly good patterns of objects that exist in nature. In addition to the simulation of natural scenes, fractal geometry can also be applied to the extraction and recognition of various image information such as biology, medical images, satellite images, and image processing and transmission in television and communications, thus forming fractal geometry and computer. A new field of research combined with graphics has moved from theoretical research to applied research [9]. Fractal solves the problem of the relationship between the whole and the part with its unique means, using the symmetry and self-similarity of the spatial structure and using various simulated real graphic leopard models, so that the entire generated scene presents the nature of infinite regression of details, richly colorful, with wonderful artistic charm. With the help of computer generation of fractals, we can generate complex natural scene graphics from a small amount of data, which brings us a big step forward in simulation [10]. It is certain that the fractal pattern has a wide range of application value in the simulation of real objects in nature, the generation of simulated shapes, computer animation, art decoration texture, pattern design, and creative production, which has attracted the attention of many scientists at home and abroad, especially graphics experts [11].

Fractal art is a form of artistic design with its own unique charm. It lacks its own perfect and powerful theoretical system for a long time. It does not establish concepts and ideas that adapt to the characteristics and development of fractal art design and does not introduce these concepts and ideas into fractal in art design. In creation and appreciation, fractal art design cannot exert its advantages and charm [12]. Furthermore, due to the troubles of technology for designers, the application of fractals in art design has been greatly hindered, which is unfavorable to the development of fractal art design itself and the whole art design [13]. Art design needs to interact with science needs to promote the rapid development of fractal art design. On the one hand, the development of science needs the support of the market, and art is an important way for scientific and technological achievements to be brought to the market and transformed into social benefits. On the other hand, the progress of design art depends on the innovation of design art means, and science just provides an unprecedented artistic means for design art [14].

Based on the special structure of fractal graphics, it will inevitably lead to the following artistic features in vision: first, the dynamic balance of fractal graphics. Generally speaking, traditional graphics pursue a static balance, and each element in fractal graphics does not exist in isolation and needs an internal dynamic to maintain it. If any element changes, it will affect the overall structure of the graph itself, thus constructing an almost completely different graph [15]. Facing the fractal graphics, viewers can feel a dynamic change that is endless and infinitely multiplying. The second is brilliant colors. Since fractal graphics are generated based on computer technology, the color of each point is generated by computer through iterative function calculation. At the same time, fractal graphics have randomness and variability, and their colors are also richer in variability and diversity. Unexpected color artistic effects are created [16].

Fractal graphics need to be modeled according to mathematical formulas and implemented using computer programming languages. Compared with traditional graphics, fractal graphics have unique modeling and decorative features [17]. However, the random form and mechanized characteristics of fractal graphics also require certain artistic treatment when they are used in pattern design. Otherwise, it will run counter to our design creation, making the pattern itself too monotonous and affecting the artistic quality of the work itself. Therefore, a good fractal art work is the product of the fusion of logical thinking and artistic feeling, that is, relying on computer operations to iterate gorgeous and regular graphics, and then supplemented by the designer's creative thinking to meet the needs of human art and aesthetic spirit [18].

2. Fractal Dynamic Model and Algorithm

2.1. Two-Dimensional Competition Model under Noise Disturbance. The dual competitor model is proposed as follows:

$$f: \begin{cases} x_{n+1} = x_n^2 - y_n^2 + c_1, \\ y_{n+1} = 2x_n y_n + c_2. \end{cases} \tag{1}$$

Among them, $x_n, y_n, c_1, c_2 \in \mathbb{R}$, which aims to describe the evolution law of x and y variables with logistic regression competition relationship. It is considered to be the most classic bivariate discrete competition model. It describes the coupling relationship between two competitors x and y under the condition of logistic regression growth law.

Considering that noise is ubiquitous in reality, the evolution of system dynamics often cannot be carried out strictly according to the iterative rules. Therefore, it is necessary to study the changing law of competitor's Bo-Yi relationship and competitor's distribution under noise interference. It is worth noting that the dynamics of continuous two-dimensional competitive systems under noise interference are reported in the top journal physical review *E*:

$$\begin{cases} \dfrac{\mathrm{d}x(t)}{dt} = \mu x(t)[1 - x(t-\tau) - \beta(t)y(t-\tau)] + x(t)\xi_x(t), \\ \dfrac{\mathrm{d}y(t)}{dt} = \mu y(v)[1 - y(t-\tau) - \beta(t)x(t-\tau)] + y(t)\xi_y(t). \end{cases} \tag{2}$$

Among them, x and y are the population density, μ is proportional to the growth rate, and $\beta(t)$ represents the interaction between species. Here $\xi_i(t)$ represents the effect of noise. In this study, Nie and Mei simulated the effect of noise and time delay on the real ecosystem at the same time and proved the following three points.

The time delay causes the two group densities to synchronously oscillate periodically; with the increase in time delay, two competitors show a transition from polystable to monostable; it is proposed that the combination of noise and time delay can provide an effective theoretical basis for understanding the real competition model.

Mandelbrot set is the key to ensure the sustainable development of competitive relationship.

In view of the importance of the parameters of the M set to the development of the competitive relationship, it is necessary to analyze its internal topological laws. However, noise is ubiquitous in reality, so that the competition relationship is often disturbed by the outside world, and the competition model is often sensitive to the initial value. Therefore, even a small external disturbance can completely change the game relationship of competitors in the future. Stochastic fractal systems have received extensive attention because they can more effectively describe the actual changing laws of competitive processes.

According to the definition, the Julia set of system (1) is the initial distribution set that guarantees the stable coexistence of two competitors x and y in the evolution process; that is, only by selecting the initial value from the Julia set the system can guarantee bounded coexistence. At the same time, it can be seen that the Mandelbrot set is a parameter set to ensure the stability of the connectivity of the attractive domain, and the good connectivity can prevent the attractive domain from collapsing when the system has a small deviation during the evolution process. Therefore, it is necessary to effectively analyze the dynamic characteristics of the parameter set of Mandelbrot set.

The P^2 point in the lattice map L is obtained as follows:

$$\theta_0 = \begin{cases} c_1 = -2 + (i-1)\left(\dfrac{4}{P-1}\right), \\ \\ c_2 = -2 + (j-1)\left(\dfrac{4}{P-1}\right). \end{cases} \tag{3}$$

Mandelbrot set $M(f)$ for noise-free mapping is shown in Figure 1.

The additive noise represented by f^a in formula (1) is defined as follows:

$$f^a = \begin{cases} x_{n+1} = x_n^2 - y_n^2 + c_1 + a_1 w_n, \\ y_{n+1} = 2x_n y_n + c_2 + a_2 w_n. \end{cases} \tag{4}$$

Among them, w_n represents the dynamic noise, and the parameter $a_1 = a_2 = a \in \mathbb{R}$ represents the intensity of the additive noise.

The multiplicative noise represented by f^m in formula (1) is defined as follows:

$$f^m = \begin{cases} x_{n+1} = (1 + m_1 w_n)x_n^2 - (1 + m_1 w_n)y_n^2 + c_1, \\ y_{n+1} = (2 + m_1 w_n)x_n y_n + c_2. \end{cases} \tag{5}$$

The parameter $m_1 = m_2 = m \in \mathbb{R}$ represents the strength of the additive noise.

Based on the escape time algorithm, $M(f_u^a)$, $M(f_u^m)$ and $M(f_n^a)$, $M(f_n^m)$ with different noise intensities a and m are shown in Figure 2. With the increase in the four kinds of noise intensity, the symmetry damage of the Mandelbrot set structure is more obvious. Additive noise destroys the M-set structure from the inside, while multiplicative noise engulfs $M(f)$ more by destroying it from the edges inward. In breaking the symmetry structure, the effect of additive noise seems to be greater than that of multiplicative noise when $a = m$.

2.2. SC and NSC. The "symmetry index" $\mathrm{sym}_{c1}(\mu_0, v_0)$ is defined as follows:

$$\mathrm{sym}_{c_1}(\mu_0, v_0) = \begin{cases} 2, & \text{If } \left|f^N(x_0, y_0, \mu_0)\right| < R \text{ And } \left|f^N(x_0, y_0, v_0)\right| < R, \\ 0, & \begin{cases} \text{If } \left|f^N(x_0, y_0, \mu_0)\right| < R \text{ And } \left|f^N(x_0, y_0, v_0)\right| \geq R, \\ \text{If } \left|f^N(x_0, y_0, \mu_0)\right| \geq R \text{ And } \left|f^N(x_0, y_0, v_0)\right| < R, \\ \text{If } \left|f^N(x_0, y_0, \mu_0)\right| \geq R \text{ And } \left|f^N(x_0, y_0, v_0)\right| \geq R. \end{cases} \end{cases} \tag{6}$$

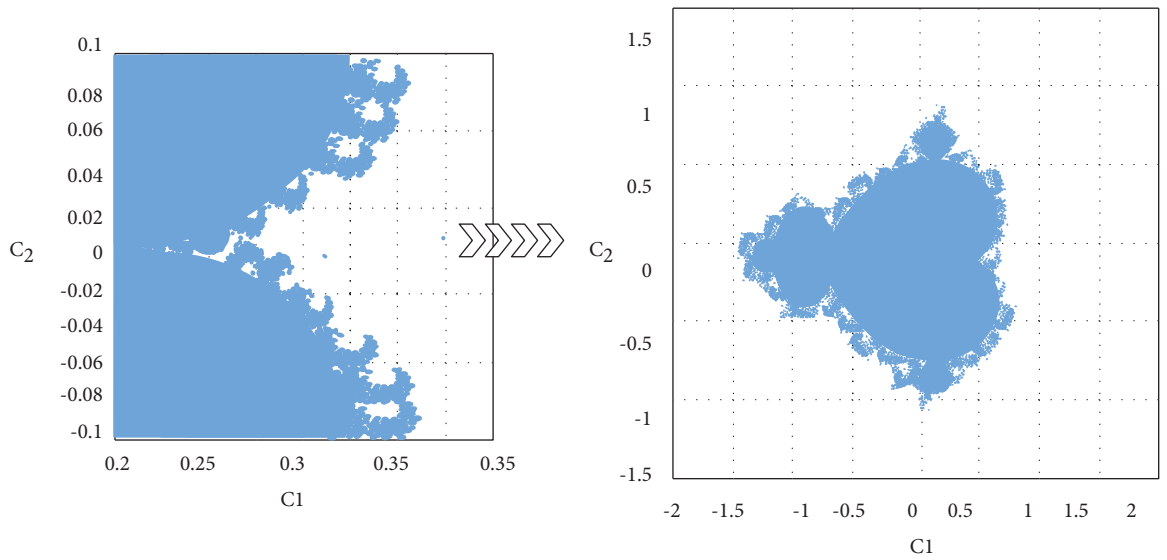

Figure 1: Mandelbrot set $M(f)$ for noise-free mapping (1).

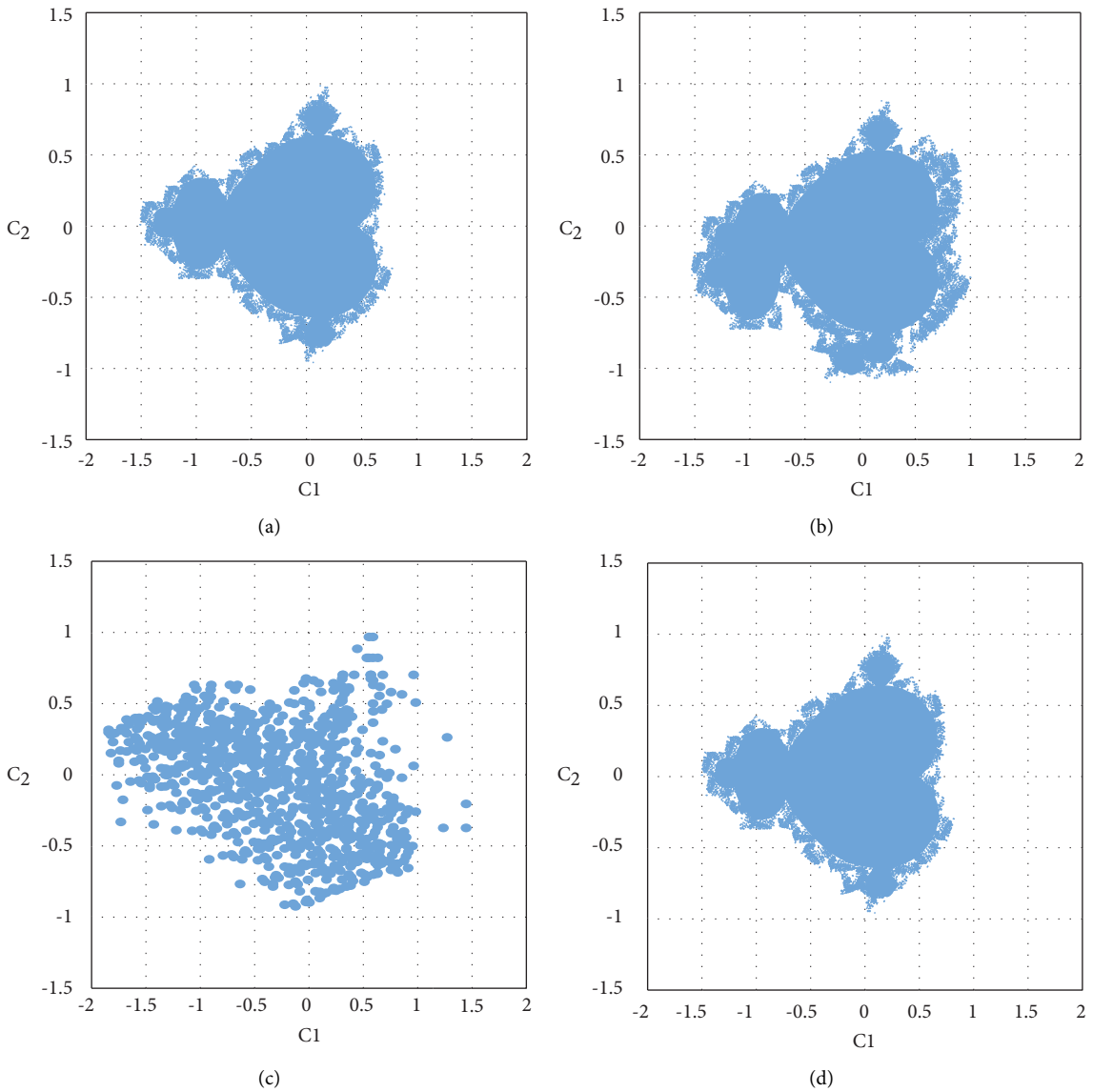

Figure 2: Continued.

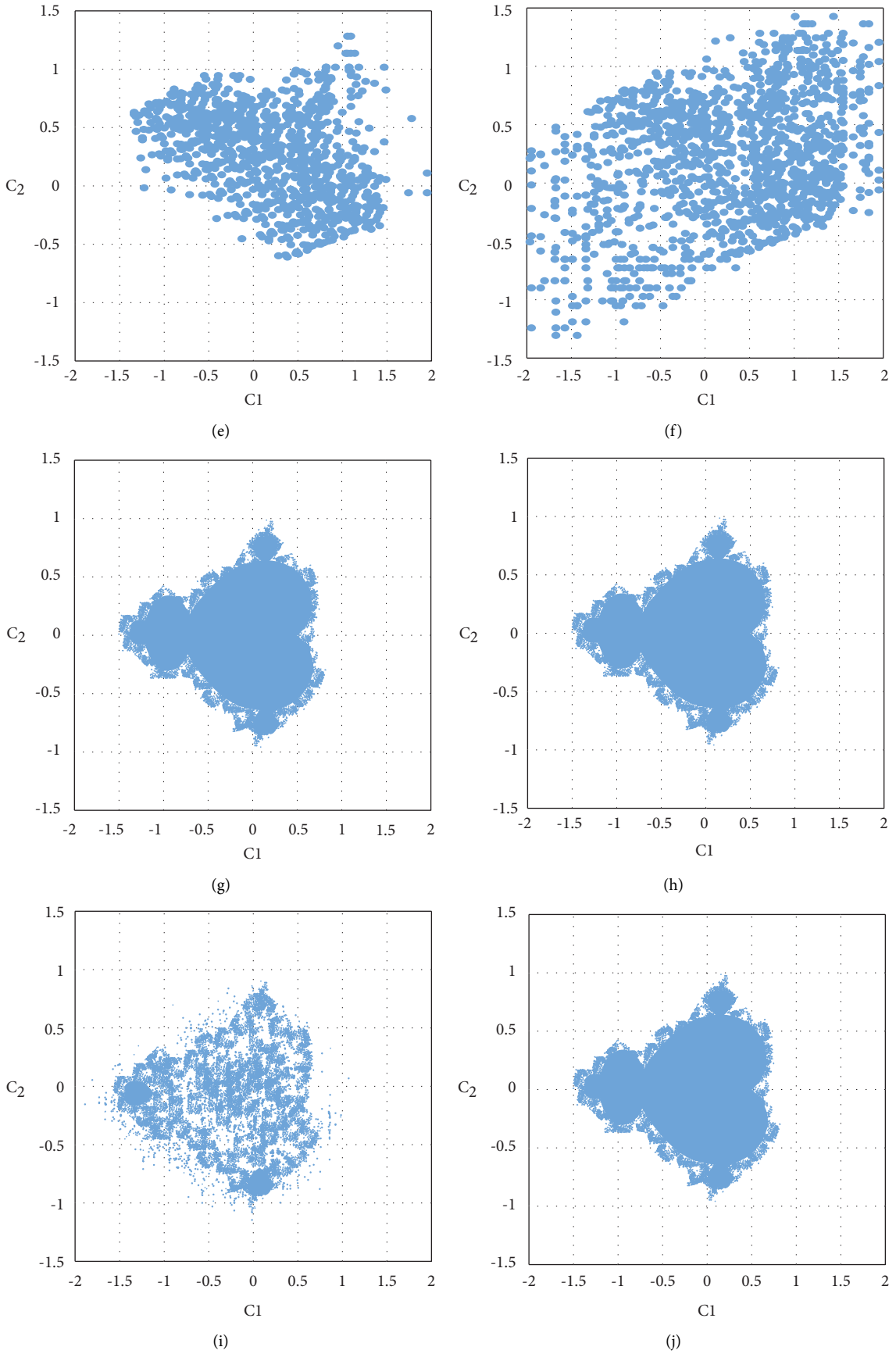

Figure 2: Continued.

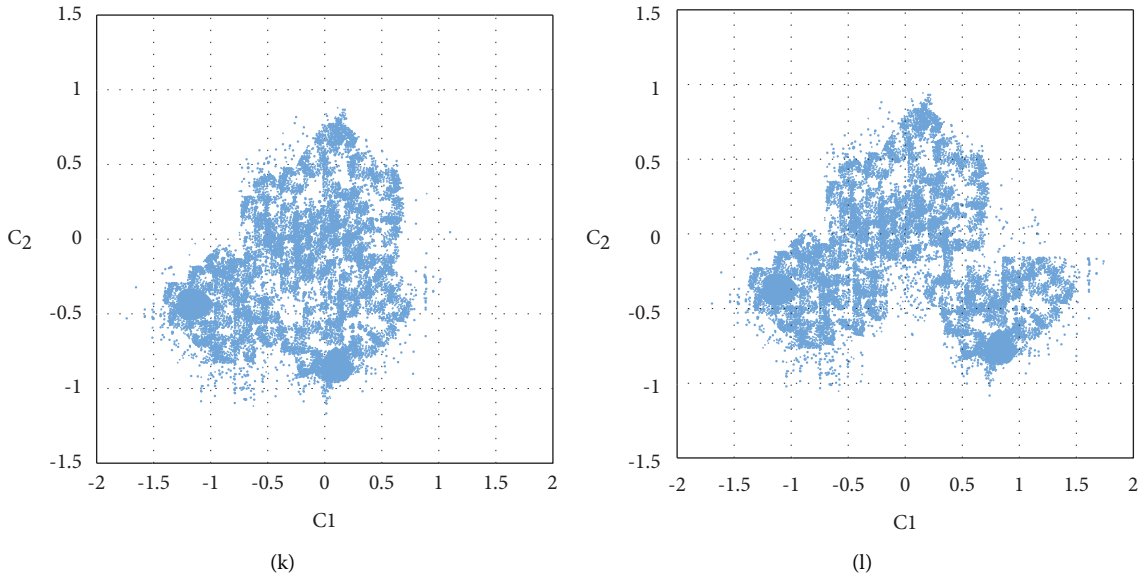

Figure 2: Mandelbrot set of noise perturbations.

$M(f_u^a)$ is denoted by $\mathrm{SC}_{c_1} M(f_u^{a_0})$.

The "Symmetry Criterion" about the c_1 axis is calculated as follows:

$$\mathrm{sym}_{c_1}(f_u^{a_0}) = \frac{1}{\mathrm{num}(M(f_u^{a_0}))} \sum_L \left(\mathrm{sym}_{c_1}(\mu_0, \nu_0)\right). \tag{7}$$

Among them, $\mathrm{num}(M(f_u^{a_0}))$ is the total number of points in $M(f_u^{a_0})$ ($\mathrm{num}(M(f_u^{a_0}))$). Obviously, $\sum_L (\mathrm{sym}_{c_1}(\mu_0, \nu_0))$ is the number of symmetry points in $M(f_u^{a_0})$. Therefore, $\mathrm{SC}_{c_1}(f_u^{a_0})$ varies in the range [0, 1]. The closer $\mathrm{SC}_{c_1}(f_u^{a_0})$ is, the more symmetrical the structure $M(f_u^{a_0})$ is.

Finally, the model calculates all the values of $\mathrm{SC}_{c_1}(f_u^{a_0})$ when $a_0 \in [0, 1]$ in increments of 0.01 and obtains the change curve of $\mathrm{SC}_{c_1}(f_u^{a_0})$.

For $w_n \sim \mathcal{U}(0, 1)$ and $w_n \sim \mathcal{N}(0, 1)$, it can be seen that $\mathrm{SC}_{c_1}(f^a)$ is larger than $\mathrm{SC}_{c_1}(f^m)$ and has the same noise intensity α. This confirms the conclusion in Figure 3.

Both $\mathrm{SC}_{c_1}(f_u)$ and $\mathrm{SC}_{c_1}(f_n)$ remain at values close to 1. That is, the noise-perturbed Mandelbrot set with more peripheral point asymmetry may have a high quantization symmetry index.

The above simulation results reveal that the peripheral points are more susceptible to noise interference because they are far from the attraction point. We show some zoomed-in details of $M(f^{a=0.8})$ in Figure 4.

The weight of SC_{c_1} of edge area points should be greater than the weight of SC_{c_1} of core area points. In Figure 4, most of the noise-perturbed Mandelbrot sets remain at [−1.5, 1.5] on the c_2 axis. Therefore, the appropriate weight of SC_{c_1}, denoted by w, can be calculated as $w = \mathrm{img}(\mu_0)/1.5|\mathrm{img}(\cdot)|$; we propose an improved "new symmetry criterion" (NSC) method as follows:

$$\mathrm{count}(\alpha_0) = \begin{cases} w, & \text{if } \left|f^N(x_0, y_0, \alpha_0)\right| < R, \\ 0, & \text{if } \left|f^N(x_0, y_0, \alpha_0)\right| \geq R. \end{cases} \tag{8}$$

For any two initial points $\mu_0 \in L_+$ and $\nu_0 \in L_-$ symmetrical about the c_1 axis, the "new symmetry index" $\mathrm{sym}_{c_1}^{Vis}(\mu_0, \nu_0)$ is defined as follows:

$$\mathrm{sym}_{c_1}^{Vis}(\mu_0, \nu_0) = \begin{cases} 2w, & \text{if } \left|f^N(x_0, y_0, \mu_0)\right| < R \text{ and } \left|f^N(x_0, y_0, \nu_0)\right| < R, \\ 0, & \text{Other cases (same as SC (symmetry criterion method)).} \end{cases} \tag{9}$$

Then, we set the "new symmetry criterion" of $M(f_u^a)$ expressed by $\mathrm{sym}_{c_1}^{Vis}(f_u^{a_0})$ about the c_1 axis to be calculated as follows:

$$\mathrm{sym}_{c_1}^{Vis}(f_u^{a_0}) = \frac{1}{\sum_L (\mathrm{count}(\alpha_0))} \sum_L \left(\mathrm{sym}_{c_1}^{Vis}(\mu_0, \nu_0)\right). \tag{10}$$

2.3. Fractal Analysis and Optimal Control of Symmetrically Coupled Three-Competitor Model. We consider system (1–1), $N = 3$ is taken, and assume that the three-competitor competition relationship presents a symmetrical coupling structure, and the following three-participant model can be obtained:

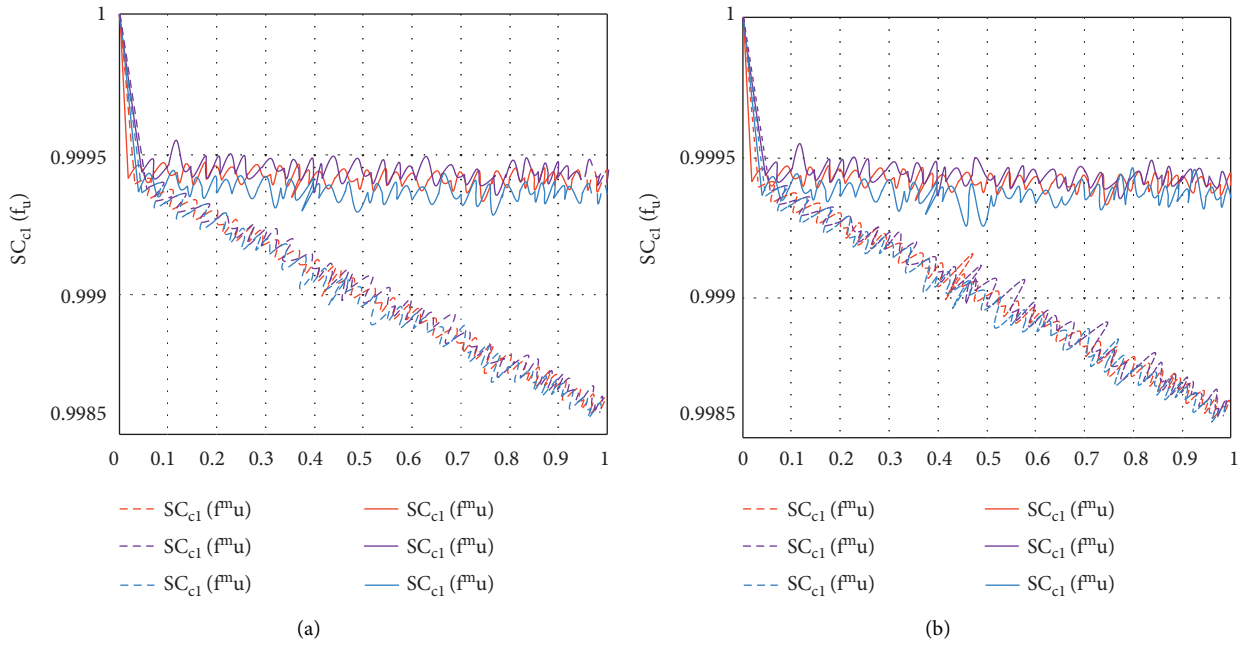

FIGURE 3: (a) $SC_{c_1}(f)$ curve and $w_n \sim \mathcal{U}(0,1)$ increase with the intensity of the reel noise: the additive noise is represented by a cool color, and the multiplicative noise is represented by a warm color. (b) The $SC_{c_1}(f)$ curve and $w_n \sim \mathcal{N}(0,1)$ increase with the noise intensity.

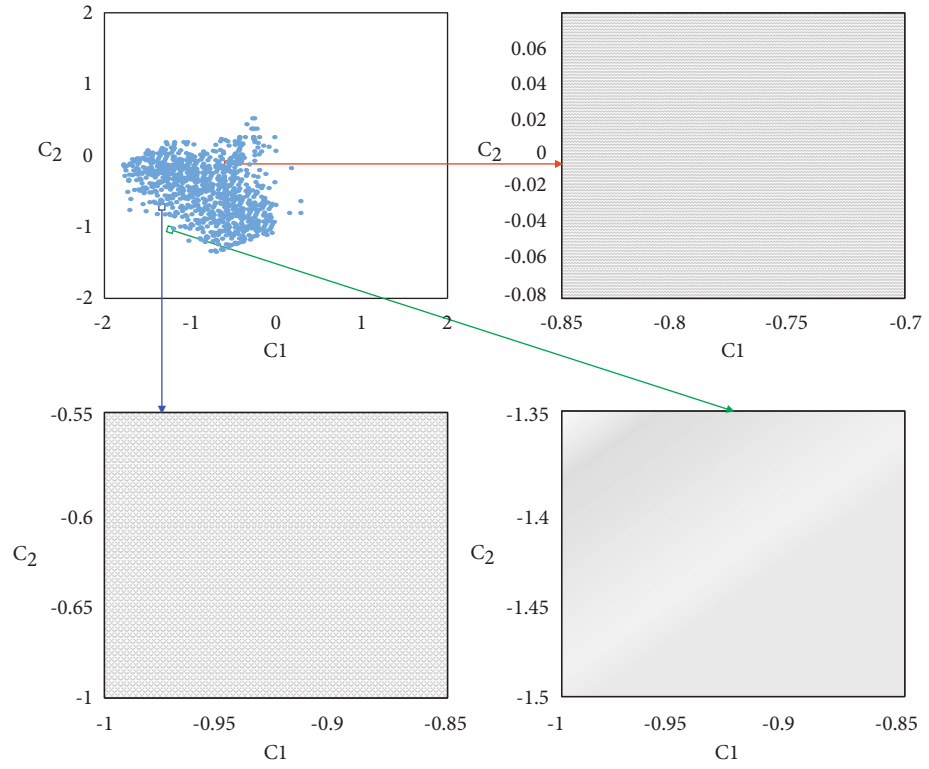

FIGURE 4: Three partial enlarged details.

$$F:\begin{cases} x_{n+1} = x_n + Rx_n(1 - x_n - \alpha y_n - \beta z_n), \\ y_{n+1} = y_n + Ry_n(1 - \beta x_n - y_n - \alpha z_n), \\ z_{n+1} = z_n + Rz_n(1 - \alpha x_n - \beta y_n - z_n). \end{cases} \tag{11}$$

When $x_i, y_i, z_i \neq 0$, we can get the fixed point $(1/1+\alpha+\beta, 1/1+\alpha+\beta, 1/1+\alpha+\beta)$, and the three competitors can coexist.

Taking parameters as $R = 1, \alpha = 0.4745$, and $\beta = 3$, the original Julia set of system (1) is shown in Figure 5. In

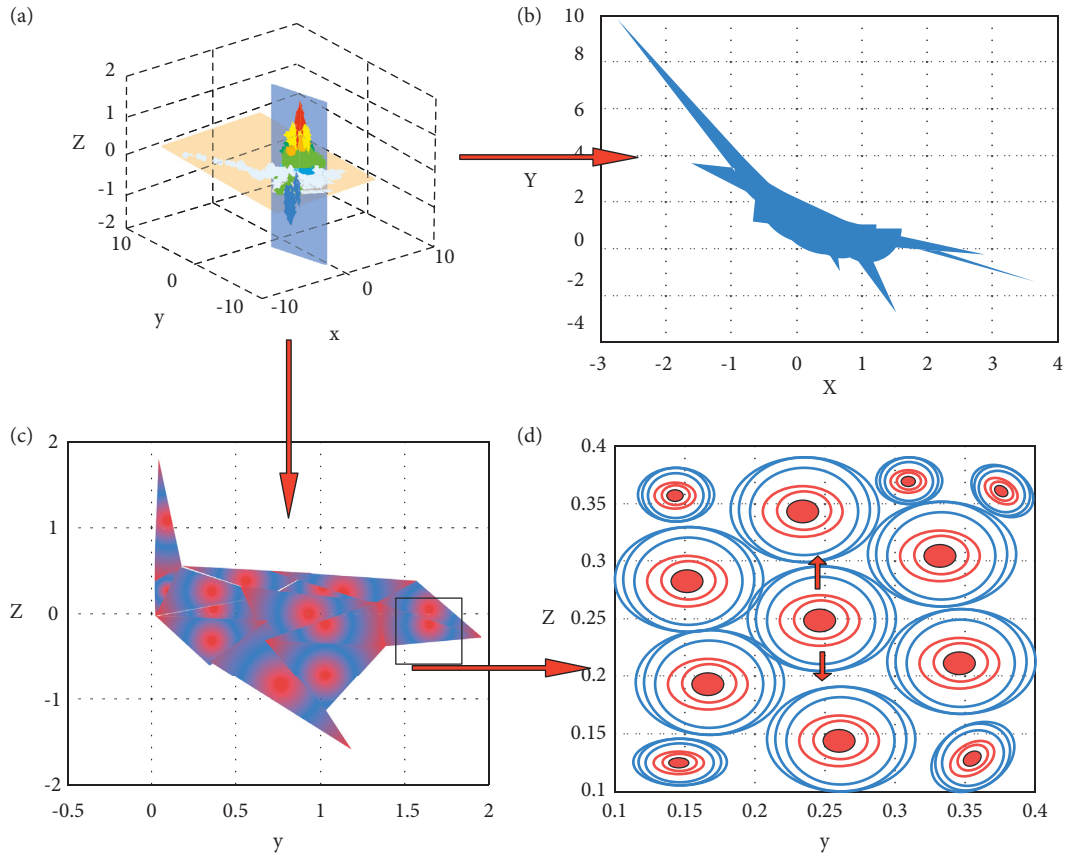

FIGURE 5: (a) Spatial Julia set $J(F)$ with $R = 1, \alpha = 0.4745$, and $\beta = 3$; (b) 2D-filled slice $K(F)$ with $z_0 = 0$; (c) 2D-filled slice K(F) with $x_0 = 0.01$; (d) local zoom of c, where we choose point $A = (0.22, 0.19) \in K(F)$ and point $B = (0.23, 0.195) \notin K(F)$.

Figure 5(b), the padding $K(F)$ with $z_0 = 0$ is shown. In fact, when one of the three competitors is eliminated, it can be regarded as a simplified case of system (1). Different initial states A and B are selected, and their competitive relationship trends are shown in Figures 6 and 7. The two figures show trajectories for $A \in K(F)$ and $B \notin K(F)$, respectively, where we can see that the trajectories remain closed until 90 iterations. However, when B's trajectory starts to deviate, the iteration continues. It can be seen from the figure that starting from the fractal attraction domain, the stable coexistence of the three competitors is guaranteed. However, the fractal attraction domain cannot guarantee the stability of the three-competitor relationship.

2.4. Optimal Control of Julia Sets for Three-Competitor Systems. By summarizing the above 8 situations, obviously, we hope that these three competitors can coexist continuously in the actual competition process. Therefore, the control process of $J(F)$ focuses on the stability of the "coexistence point" $(1/1 + \alpha + \beta, 1/1 + \alpha + \beta, 1/1 + \alpha + \beta)$; to keep the fixed point constant, we apply the following gradient optimization controls:

$$\begin{cases} u_{n1} = -\dfrac{k}{1+k}\left(f(x_n, y_n, z_n) - x^*\right), \\ u_{n2} = -\dfrac{k}{1+k}\left(g(x_n, y_n, z_n) - y^*\right), \\ u_{n3} = -\dfrac{k}{1+k}\left(q(x_n, y_n, z_n) - z^*\right). \end{cases} \tag{12}$$

Since $x^* = y^* = z^* = 1/1 + \alpha + \beta$, by adding control term (2) to system (1), the following optimized system can be obtained:

$$P: \begin{cases} x_{n+1} = \dfrac{1}{1+k}\left(f(x_n, y_n, z_n) + \dfrac{k}{1+k}x^*\right), \\ y_{n+1} = \dfrac{1}{1+k}\left(g(x_n, y_n, z_n) + \dfrac{k}{1+k}x^*\right), \\ z_{n+1} = \dfrac{1}{1+k}\left(q(x_n, y_n, z_n) + \dfrac{k}{1+k}x^*\right). \end{cases} \tag{13}$$

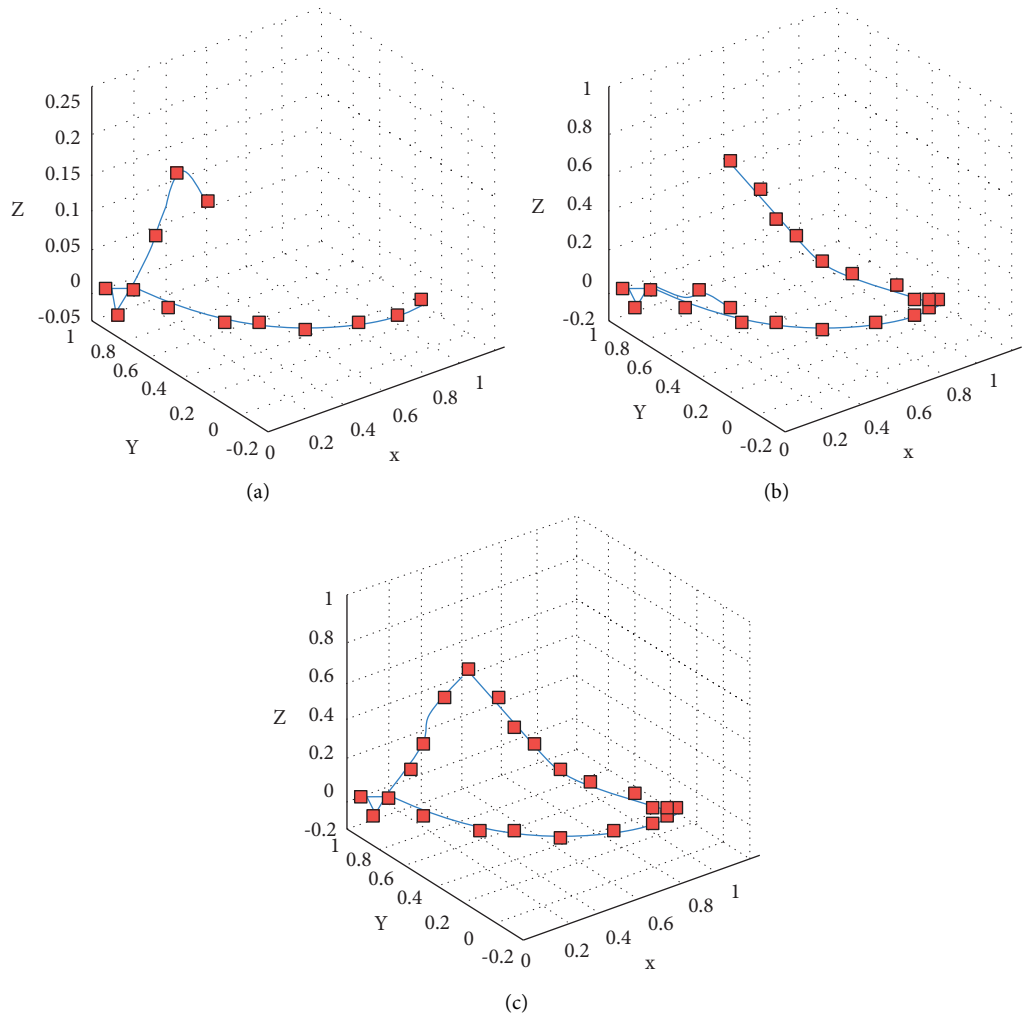

Figure 6: Competitive relationship trajectory of A ((a) 20 iterations; (b) 40 iterations; (c) 100 iterations).

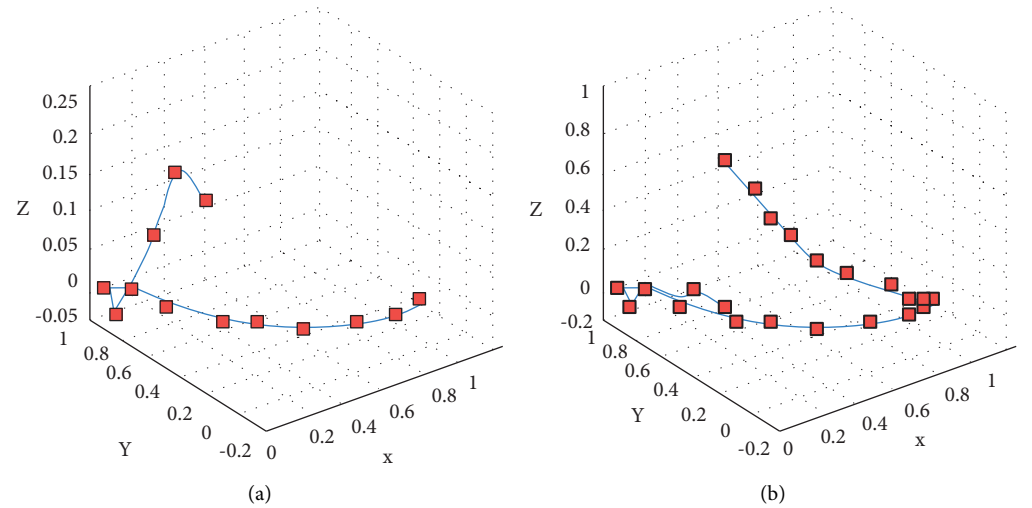

Figure 7: Continued.

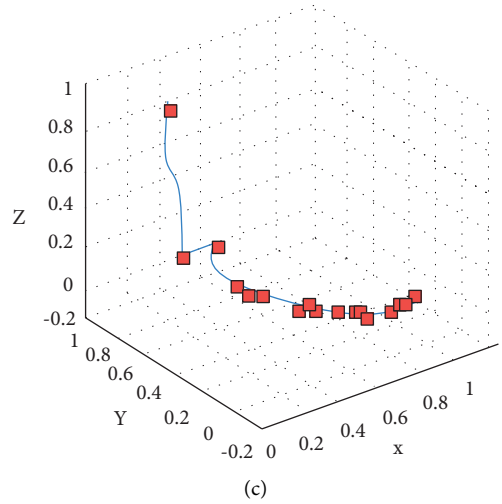

Figure 7: Competitive relationship trajectory of B ((a) 20 iterations; (b) 40 iterations; (c) 91 iterations).

Based on the above analysis, $J(F)$ is the domain of attraction that attracts fixed points. Therefore, by adding a control term, it is possible to control the Julia set in which the distribution density of the three competitors remains stable by affecting the iterative trajectory of the initial point in system (3), while achieving the stability of the fixed point.

The Jacobi matrix of system (3) at the fixed point $(x^*, y^*, z^*) = (1/1+\alpha+\beta, 1/1+\alpha+\beta, 1/1+\alpha+\beta)$ is considered as follows:

$$J = \begin{bmatrix} \frac{1+R}{1+k} - \frac{2R}{1+k}x^* - \frac{\alpha R}{1+k}y^* - \frac{\beta R}{1+k}z^* & -\frac{\alpha R}{1+kx^*\alpha^*} & \\ -\frac{\beta R}{1+k}y^* & \frac{1+R}{1+k} - \frac{2R}{1+k}y^* - \frac{\alpha R}{1+k}z^* - \frac{\beta R}{1+k}x^* & -\frac{\beta R}{1+k}x^* \\ -\frac{\alpha R}{1+k}z^* & -\frac{\alpha R}{1+k}z^* & \frac{1+R}{1+k} - \frac{2R}{1+k}z^* - \frac{\alpha R}{1+k}x^* - \frac{\beta R}{1+k}y^* \end{bmatrix}. \quad (14)$$

The characteristic formula of the Jacobi matrix J is expressed as follows:

$$\Delta(\lambda) = \lambda^3 + \widetilde{P}\lambda^2 + \widetilde{Q}\lambda + \widetilde{S} = 0. \quad (15)$$

At this point, there are

(1) $T = (2+\alpha+\beta)Rx^* - (1+R)$

(2) $\widetilde{P} = 3T/1+k$

(3) $\widetilde{Q} = 3T^2 - 3\alpha\beta R^2 x^{*2}/(1+k)^2$

(4) $\widetilde{S} = T^3 - \alpha^3 R^3 x^{*3} - \beta^3 R^3 x^{*3} - 3T\alpha\beta R^2 x^{*2}/(1+k)^3$

To determine that the controlled system (1) is stable at fixed points $(1/1+\alpha+\beta, 1/1+\alpha+\beta, 1/1+\alpha+\beta)$, the following three conditions need to be satisfied:

(1) $\Delta(1) > 0.\Delta(1) = 1 + \widetilde{P} + \widetilde{Q} + \widetilde{S} > 0$

(2) $1 - \widetilde{P} + \widetilde{Q} - \widetilde{S} > 0$

(3) $|\widetilde{S}| < 1$ and $|\widetilde{S}^2 - 1| > |\widetilde{S}\widetilde{P} - \widetilde{Q}|$

For two-competitor and multiple-competitor systems, the complex coupling behavior between competitors increases the difficulty of analyzing the topological properties of Julia sets.

It simplifies to a competing behavior involving chain coupling, as follows:

$$F_{x_1x_2x_3}\begin{cases} x_{1_{n+1}} = x_{1_n} + Rx_{1_n}\left(1 - x_{1_n} - \alpha x_{2_n} - \beta x_{3_n}\right), \\ x_{2_{n+1}} = x_{2_n} + Rx_{2_n}\left(1 - \alpha x_{3_n} - x_{2_n}\right), \\ x_{3_{n+1}} = x_{3_n} + Rx_{3_n}\left(1 - x_{3_n}\right). \end{cases} \quad (16)$$

Among them, R, α, β have the same meaning as system (3), x_1, x_2, x_3 represent three competitors, respectively, which means that x_1 to x_3 are a progressive competition relationship. Among them, x_3 is the highest level competitor, that is, the single-headed competitor. Its competitiveness is stronger than that of x_1 and x_2, and the competitiveness of x_2 is stronger than that of R.

The upper bound of the $J(F_{x_1x_2x_3})$ system is given by the following theorem.

Theorem 1. *We have*

$$J\left(F_{x_1x_2x_3}\right) \subset \left\{\left(x_{1_0}, x_{2_0}, x_{3_0}\right)\middle| i_0\right| < B_i, i = x_1, x_2, x_3\right\}. \quad (17)$$

Among them, $B_{x_3} = |R+1|/|R|, B_{x_2} = |R+1| + |R\alpha B_{x_3}|/|R|, B_{x_1} = |R+1| + |R\alpha B_{x_2}| + |R\beta B_{x_3}|/|R|$.

The proof is as follows.

For x_3 without a stronger competitor, if $|x_{3_0}| > |R+1|/|R|$, we can get the following:

$$\left|x_{3_1}\right| \geq \left|x_{3_0}\right|^2 - R - \left|x_{3_0}\right|(|1+R|). \tag{18}$$

At this time, $\exists\epsilon$ makes $\lim_{n\longrightarrow\infty}(1+\epsilon)^n|x_{3_0}| \longrightarrow \infty$, so $|x_{3_0}| < |R+1|/|R|$ is a necessary condition to make $J(F_{x_1x_2x_3})$ bounded. If $|x_{2_0}| \geq B_{x_2}$, we can get the following:

$$\begin{aligned}\left|x_{2_1}\right| &= \left|(1+R)x_{2_0} - Rx_{2_0}^2 - R\alpha x_{3_0}x_{2_0}\right| \\ &\geq |R|\left|x_{2_0}\right|^2 - \left(|1+R|x_{2_0} + |R\alpha|\left|x_{3_0}\right|\left|x_{2_0}\right|\right) \\ &\geq |R|\left|x_{2_0}\right|^2 - \left(|1+R| + \left|R\alpha B_{x_3}\right|\right)x_{2_0}.\end{aligned} \tag{19}$$

At this time, $\exists\epsilon$ makes $\lim_{n\longrightarrow\infty}|x_{2_{n+1}}| = \lim_{n\longrightarrow\infty}(1+\varepsilon)^n|x_{2_0}| \longrightarrow \infty$, so obviously $|x_{2_0}| < B_{x_2}$ is a necessary condition to make $J(F_{x_1x_2x_3})$ bounded. Likewise, if $|x_{1_0}| > B_{x_1}$, we can get the following:

$$\begin{aligned}\left|x_{1_1}\right| &= \left|(1+R)x_{1_0} - Rx_{1_0}^2 - R\alpha x_{2_0}x_{1_0}\right| \\ &\geq |R|\left|x_{1_0}\right|^2 - \left|x_{1_0}\right|\left(|1+R| + \left|R\alpha B_{x_2}\right| + \left|R\beta B_{x_3}\right|\right).\end{aligned} \tag{20}$$

At this time, $\exists\epsilon$ makes $\lim_{n\longrightarrow\infty}|x_{1_{n+1}}| = \lim_{n\longrightarrow\infty}(1+\varepsilon)^n|x_{1_0}| \longrightarrow \infty$, so obviously $|x_{1_0}| < B_{x_1}$ is a necessary condition to make $J(F_{x_1x_2x_3})$ bounded.

2.5. Synchronization of Julia Sets for Three-Competitor Systems. Synchronization is considered as another optimal control method, whose purpose is to make the dynamics of the controlled system behave the same as the ideal system. For the purposes of this section, synchronization aims to steer a competitive relationship with a specified steady state. Synchronization of Julia sets can be achieved by adding some coupling terms. System (4) with the same structure as system (3) but with different parameters is considered as follows:

$$\widetilde{F}:\begin{cases} u_{n+1} = u_n + \widetilde{R}u_n\left(1 - u_n - \widetilde{\alpha}v_n - \widetilde{\beta}w_n\right), \\ v_{n+1} = v_n + \widetilde{R}v_n\left(1 - \widetilde{\beta}u_n - v_n - \widetilde{\alpha}w_n\right), \\ w_{n+1} = w_n + \widetilde{R}w_n\left(1 - \widetilde{\alpha}u_n - \widetilde{\beta}v_n - w_n\right). \end{cases} \tag{21}$$

To relate system (5) to the ideal system (3), we introduce two coupling terms in it to get the following:

$$\widetilde{F}^0:\begin{cases} u_{n+1} = 2u_n - u_n^2 - \widetilde{\alpha}u_nv_n - \widetilde{\beta}u_nw_n - L_1(u_n - x_n) \\ \quad -\widetilde{L}_1\left(\beta x_nz_n + \alpha x_ny_n + x^2 - \widetilde{\beta}u_nv_n - \widetilde{\alpha}u_nv_n - u_n^2\right), \\ v_{n+1} = 2v_n - v_n^2 - \widetilde{\alpha}u_nw_n - \widetilde{\beta}u_nv_n - L_2(v_n - y_n) \\ \quad -\widetilde{L}_2\left(\beta x_ny_n + \alpha y_nz_n + y^2 - \widetilde{\beta}u_nv_n - \widetilde{\alpha}v_nw_n - v_n^2\right), \\ w_{n+1} = 2w_n - w_n^2 - \widetilde{\alpha}u_nw_n - \widetilde{\beta}v_nw_n - L_3(w_n - z_n) \\ \quad -\widetilde{L}_3\left(\beta y_nz_n + \alpha x_nz_n + z^2 - \widetilde{\beta}v_nw_n - \widetilde{\alpha}u_nw_n - w_n^2\right). \end{cases} \tag{22}$$

The Julia sets of systems (6) and (3) are denoted as $J(\widetilde{F}^0)$ and $J(F)$, respectively, and the unified expression L of the coupling parameters L_j and $\widetilde{L}_j$ $(j = 1, 2, 3)$ is given, and the following lemmas and theorems are obtained.

Lemma 1. *If there is some L_0 satisfying the following formula, it is said to achieve synchronization between $J(\widetilde{F}^0)$ and J(F).*

$$\lim_{L\longrightarrow L_0}\left(J\left(\widetilde{F}^O\right) \cup J(F) - J\left(\widetilde{F}^O\right) \cap J(F)\right) = \varnothing. \tag{23}$$

Theorem 2. *$J(\widetilde{F})$ and J(F) are synchronized when $L_i \longrightarrow 1, \widetilde{L}_l \longrightarrow 2$.*

The proof is as follows.

Obviously, the Julia set is obtained by iterating over points within a bounded region, which is denoted by Ω. Since $\psi_0 \notin J(F)$, the presence of n_0 will cause $F^{n_0}(\psi_0)$ to escape from the Ω region. Therefore, in the synchronization process, only the points of the trajectory within Ω need to be considered. Therefore, $\exists N_1$ makes $|\beta||x_nz_n| + |\widetilde{\beta}||u_nw_n| < N_1, |\alpha||x_ny_n| + |\alpha||u_nv_n| < N_1, |x_n^2| + |u_n^2| < N_1$.

Then, we have the following:

$$\begin{aligned}\left|u_{n+1} - x_{n+1}\right| &\leq \left|Z - L_1\right|\left|u_n - x_n\right| + \left|1 - \widetilde{L}_1\right|\left|\alpha x_ny_n - \widetilde{\alpha}x_ny_n\right| + \left|1 - \widetilde{L}_1\right|\left|\beta x_ny_n - \widetilde{\beta}u_nw_n\right| + \left|1 - \widetilde{L}_1\right|\left|x_n^2 - u_n^2\right| \\ &\leq \left|2 - L_1\right|\left|u_n - x_n\right| + \left|1 - \widetilde{L}_1\right|\left(|\beta|\left|x_nz_n\right| + |\widetilde{\beta}|\left|u_nw_n\right|\right) + \left|1 - \widetilde{L}_1\right|\left(|\alpha|\left|x_ny_n\right| + |\widetilde{\alpha}|\left|u_nv_n\right|\right) + \left|1 - \widetilde{L}_1\right|\left(x_n^2 + u_n^2\right) \\ &\leq \left|2 - L_1\right|\left|u_n - x_n\right| + 3\left|1 - \widetilde{L}_1\right|N_1 \\ &\leq \left|2 - L_1\right|\left(\left|2 - L\_1\right|\left|u\_\{n-1\} - x\_\{n-1\}\right| + 3\left|1 - \widetilde{L}_1\right|N_1\right) + 3\left|1 - \widetilde{L}_1\right|N_1 \\ &\leq \left|2 - L_1\right|^2\left|u_{n-1} - x_{n-1}\right| + 3\left|1 - \widetilde{L}_1\right|N_1\left(1 + \left|2 - L_1\right|\right) \\ &\leq \cdots\cdots \\ &\leq \left|2 - L_1\right|^n\left|u_1 - x1\right| + 3\left|1 - \widetilde{L}_1\right|N_1\left(1 + \left|2 - L_1\right| + \left|2 - L_1\right|^2 + \cdots + \left|2 - L_1\right|^n\right) \\ &= \left|2 - L_1\right|^n\left|u_1 - x_1\right| + 3\left|1 - \widetilde{L}_1\right|N_1\frac{1 - \left|2 - L_1\right|^n}{1 - \left|2 - L_1\right|}.\end{aligned} \tag{24}$$

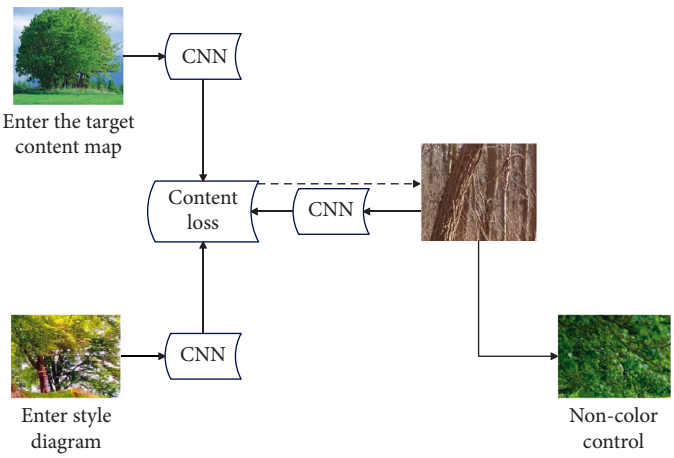

Figure 8: CAD fractal art pattern design system fused with RBF neural network algorithm.

That is, $|u_{n+1} - x_{n+1}| \le |2 - L_1|^n |u_1 - x_1| + 3|1 - \widetilde{L}_1|N_1 1 - |2 - L_1|^n / 1 - |2 - L_1|$, the right side constraint satisfies $L_1 \longrightarrow 2$, and the trajectories of $\widetilde{L}_1 \longrightarrow 1, u_n$, and x_n are synchronized. It can also be concluded that when $L_{2,3} \longrightarrow 2, \widetilde{L}_{2,3} \longrightarrow 1$, the trajectories of v_n, y_n, w_n, z_n are synchronized.

The algorithm camouflages the artistic style using a masked image pattern by controlling the style of the artistic pattern design on the spatial domain. Figure 8 is a comprehensive flow chart of artistic pattern design, and mask image and color controls are optional. If the mask image is invalid, the style transfer can be performed without spatial region control.

3. Simulation Test

After extracting the artistic pattern features, when searching, the algorithm will extract the artistic pattern features of the image to be retrieved and then compare them with the artistic pattern features of the image art pattern feature library. There are many factors that affect the retrieval results, such as the amount of image dimensionality reduction and the similarities and differences in similarity matching algorithms. These will more or less have a certain impact on the accuracy of the retrieval results. In view of these factors, this study studies their influence on the retrieval results. Because the classification of images is not involved in this article, the data used in the experiments are image sets with high similarity. The experimental results of nonequal scaling experiments are shown in Table 1.

From Table 1, it can be seen that the model proposed in this study has a good performance in nonequal scaling. On this basis, the effect of the CAD fractal art pattern design system based on the RBF neural network algorithm proposed in this study is verified, and the fractal art pattern design effect is calculated, as shown in Table 2.

It can be seen from the above research that the CAD fractal art pattern design system based on the RBF neural network algorithm proposed in this study has a good effect on fractal art pattern design.

Table 1: Experimental results of nonequal scaling.

Compression ratio	Image size after compression	Average value of images related to search results	Average retrieval accuracy (%)
0.071×0.16	56.0×56.0	3.774	38
0.0976×0.147	78.0×78.0	3.978	40
0.1126×0.168	90.0×90.0	4.488	55
0.142×0.213	112.0×112.0	7.344	73
0.226×0.337	180.0×180.0	8.262	83
0.281×0.423	224.0×224.0	9.282	93
0.376×0.566	300.0×300.0	9.078	91
0.643×0.962	512.0×512.0	9.18	92

Table 2: Design effects of fractal art patterns.

Number	Design effect	Number	Design effect	Number	Design effect
1	86.712	11	85.358	21	84.778
2	90.046	12	84.257	22	89.849
3	85.341	13	90.895	23	84.137
4	90.363	14	89.663	24	84.683
5	87.326	15	85.738	25	85.313
6	87.915	16	87.062	26	90.072
7	89.522	17	88.967	27	86.017
8	89.825	18	88.082	28	88.070
9	87.661	19	87.515	29	86.369
10	87.530	20	86.929	30	85.330

4. Conclusion

Fractals are everywhere, and fractal theory is called the geometry of nature, which is essentially a new worldview and methodology. Moreover, it can be used for reference by other disciplines and has penetrated into many disciplines including physics, chemistry, biomedicine, materials science, economic management, and computer graphics. In addition, the fractal theory has broad application prospects. While promoting research in related fields, it also brings forward many new topics that need further

research. At present, fractals, especially fractal patterns, are gradually entering people's lives. People are not only limited to appreciating the wonderful fractal art, but have begun to consciously bring fractals into industrial design. This study combines the RBF neural network algorithm to design and evaluate the CAD fractal art pattern to improve the effect of fractal art pattern design. The experimental results show that the CAD fractal art pattern design system based on the RBF neural network algorithm proposed in this study has a good effect on fractal art pattern design.

Data Availability

The labeled datasets used to support the findings of this study are available from the corresponding author upon request.

Conflicts of Interest

The authors declare no conflicts of interest.

References

[1] G. Yi, "Design research on the network multimedia courseware for art-design teaching," *Eurasia Journal of Mathematics, Science and Technology Education*, vol. 13, no. 12, pp. 7885–7892, 2017.

[2] Q. Wan, S. S. Song, X. H. Li et al., "The visual perception of the cardboard product using eye-tracking technology," *Wood Research*, vol. 63, no. 1, pp. 165–178, 2018.

[3] N. McCartney and J. Tynan, "Fashioning contemporary art: a new interdisciplinary aesthetics in art-design collaborations," *Journal of Visual Art Practice*, vol. 20, no. 1-2, pp. 143–162, 2021.

[4] J. Lockheart, "The importance of writing as a material practice for art and design students: a contemporary rereading of the Coldstream Reports," *Art, Design and Communication in Higher Education*, vol. 17, no. 2, pp. 151–175, 2018.

[5] G. Sachdev, "Engaging with plants in an urban environment through street art and design," *Plants, People, Planet*, vol. 1, no. 3, pp. 271–289, 2019.

[6] Y. M. Andreeva, V. C. Luong, D. S. Lutoshina et al., "Laser coloration of metals in visual art and design," *Optical Materials Express*, vol. 9, no. 3, p. 1310, 2019.

[7] Z. Nebessayeva, K. Bekbolatova, K. Mussakulov, S. Zhanbirshiyev, and L. Tulepov, "Promotion of entrepreneurship development by art and design by pedagogy," *Opción*, vol. 34, no. 85-2, pp. 729–751, 2018.

[8] D. Mourtzis, "Simulation in the design and operation of manufacturing systems: state of the art and new trends," *International Journal of Production Research*, vol. 58, no. 7, pp. 1927–1949, 2020.

[9] K. W. Klockars, N. E. Yau, B. L. Tardy et al., "Asymmetrical coffee rings from cellulose nanocrystals and prospects in art and design," *Cellulose*, vol. 26, no. 1, pp. 491–506, 2019.

[10] M. Hermus, A. van Buuren, and V. Bekkers, "Applying design in public administration: a literature review to explore the state of the art," *Policy & Politics*, vol. 48, no. 1, pp. 21–48, 2020.

[11] J. Calvert and P. Schyfter, "What can science and technology studies learn from art and design? Reflections on 'Synthetic Aesthetics," *Social Studies of Science*, vol. 47, no. 2, pp. 195–215, 2017.

[12] E. Knight, J. Daymond, and S. Paroutis, "Design-led strategy: how to bring design thinking into the art of strategic management," *California Management Review*, vol. 62, no. 2, pp. 30–52, 2020.

[13] D. Jordan and H. O'Donoghue, "Histories of change in art and design education in Ireland: towards reform: the evolving trajectory of art education," *International Journal of Art and Design Education*, vol. 37, no. 4, pp. 574–586, 2018.

[14] T. Bastogne, "Quality-by-design of nanopharmaceuticals–a state of the art," *Nanomedicine: Nanotechnology, Biology and Medicine*, vol. 13, no. 7, pp. 2151–2157, 2017.

[15] K. Maras, "A realist account of critical agency in art criticism in art and design education," *International Journal of Art and Design Education*, vol. 37, no. 4, pp. 599–610, 2018.

[16] M. S. Ravelomanantsoa, Y. Ducq, and B. Vallespir, "A state of the art and comparison of approaches for performance measurement systems definition and design," *International Journal of Production Research*, vol. 57, no. 15-16, pp. 5026–5046, 2019.

[17] K. C. Tsai, "Teacher-student relationships, satisfaction, and achievement among art and design college students in Macau," *Journal of Education and Practice*, vol. 8, no. 6, pp. 12–16, 2017.

[18] H. Liu, X. T. Zhang, X. M. Fu, Z. C. Dong, and L. Liu, "Computational peeling art design," *ACM Transactions on Graphics*, vol. 38, no. 4, pp. 1–12, 2019.